

# Interference in Wireless Multi-hop Ad-hoc Networks and its Effect on Network Capacity

R. Hekmat and P. Van Mieghem  
Delft University of Technology  
Information Technology and Systems  
P.O. Box 5031, 2600 GA Delft, The Netherlands  
Email: R.Hekmat@its.tudelft.nl, P.VanMieghem@its.tudelft.nl

**Abstract**—In this paper we propose a new model to calculate interference levels in wireless multi-hop ad-hoc networks. This model computes the expected value of Carrier to Interference ratio ( $C/I$ ) by taking into account the number of nodes, density of nodes, radio propagation aspects, multi-hop characteristics of the network, and the amount of relay traffic. The expected values of  $C/I$  are used to determine network capacity and data throughput per node.

Our model uses a regular lattice for possible locations of mobile nodes. This enables us to calculate the expected values of  $C/I$ , without having detailed information about movement patterns and exact location of all nodes at any moment. Based on this model we have evaluated effects of variations in the network size, network density and traffic load on  $C/I$ , and consequently throughput of the network. Our calculations suggest that interference is upper-bounded in wireless ad-hoc networks that use carrier sensing for medium access control. Further, from the point of view of throughput optimization, our calculations show limits on the network size and input data rates per node.

## I. INTRODUCTION

In wireless ad-hoc networks communication between nodes takes place over radio channels. As long as all nodes use the same frequency band for communication, any node-to-node transmission will add to the level of interference experienced by other users. Variations in network size (number of nodes), network density (relative positions of nodes) and traffic per node could have strong influence on interference experienced by mobile nodes throughout the network. It is well known that radio channel capacity decreases as the wanted signal carrier power to interference ratio ( $C/I$ ) decreases<sup>1</sup>. Therefore, for performance evaluation of mobile wireless ad-hoc networks, it is important to have good estimates of interference levels.

To our knowledge little work has been carried out on the analytic modeling of the expected values of carrier to interference ratio in wireless multi-hop ad-hoc networks. Consequently, fundamental properties and limitations of ad-hoc networks, from radio interference point of view, have remained unpublished yet. The IETF working group MANET [1] is concentrating mostly on routing protocols and their optimization. But in proposed protocols (e.g. [2], [3]) each node acts according to its local traffic without considering possible inference from other nodes or towards other nodes. Valuable papers have been published where different routing protocols and different access

technologies are compared qua performance, stability and scalability ([4]-[7]). However, these comparisons are mostly based on simulations or in some occasions on field trial measurement results. Hardly any mathematical modeling is used. Simulation results and measurements, although extremely useful, are often limited in scope and fail to provide in depth understanding of system dependencies on varying parameters.

In [8], the scalability of routing protocols designed for ad-hoc networks is studied, and indeed an analytic framework is suggested. However, this paper does not include the influence of radio interference on the performance of routing protocols. In [9], a theoretical study is presented for bandwidth reservation in ad-hoc networks in the presence of interference, but carrier to interference ratio and the link between changing network parameters and interference levels is not considered. In [10], the capacity of a wireless ad-hoc network is determined by taking into consideration the relay traffic from an arbitrary source to any destination. However, this study is restricted to that case where there is only one active source-destination pair.

Power saving schemes and energy efficient routing methods for multi-hop ad-hoc networks are studied in various papers e.g. [11] and [12], but again the possibility of signal loss due to radio interference and its effect on power consumption at mobile nodes is not included in these studies.

In this paper we propose a new model for calculation of interference levels in wireless multi-hop ad-hoc networks. This model takes into account the number of nodes, density of nodes, multi-hop characteristics of the network, and relay traffic. The expected values of  $C/I$  are used to determine radio channel capacity and useful data output rates (throughput) per node.

In mobile ad-hoc networks users could move around freely at all times. Therefore, one may expect that finding good estimations for  $C/I$  would require access to accurate information regarding movement patterns and the exact location of all nodes at any moment. Our model in this paper uses a regular lattice for possible locations of mobile nodes. This may seem contradictory to the complete freedom of movement of nodes in ad-hoc networks. Yet, we show that introduction of the regular lattice simplifies computations and allows us to calculate an upper bound on the expected values of  $C/I$  that also holds for moving nodes with random positions.

The structure of this article is as follows. In section II we describe our model. Interference levels in ad-hoc networks de-

<sup>1</sup>See for example [15, Chapter 8]

depends not only on generated new traffic per node, but also on relay traffic that is hopping from source to destination throughout the network. The amount of relay traffic in an ad-hoc network depends directly on the number of hops from any arbitrary source to any other destination. We compute in section III the exact hop distribution in our proposed model. In section IV we show the relation between the mean value of traffic per node (the sum of a node's own traffic and traffic relayed by that node) and the average hopcount. In section V we derive a formula for computation of the expected values of carrier to interference ratio as function of the network size, network density and traffic per node. In section VI we focus on capacity of wireless ad-hoc networks and analyze effects of variation in overall network size, network density and input traffic on data through per node. In section VII we evaluate our model critically. We summarize our conclusions in section VIII.

## II. MODEL DESCRIPTION

In this section we describe our model for a multi-hop ad-hoc network. We will discuss in the remainder of this report how this model facilitates analytic computation of the hopcount, traffic per node and the expected value of carrier to interference ratio.

### A. Model assumptions and definitions

The main assumptions that form the basis for our model and our calculation of interference are described in sections II-A.1 to II-A.4.

1) *Radio model*: Our interference calculations in this paper will be based on the path-loss power law model for radio propagation [17]. According to this model, the mean value of received signal power indicated by  $p_a$  (in Watts) is a decreasing function of distance  $d$  between the transmitter and the receiver and can be represented as:

$$p_a = c \cdot d^{-\eta} \quad (1)$$

where  $c$  is a constant that depends on transmitted power, the receiver and the transmitter antenna gains and the wavelength [17];  $\eta$  is the path loss exponent and varies between 2 and 6 depending on the radio propagation environment<sup>2</sup>. Higher values for  $\eta$  indicate faster decay of radio signals. This simple model does not include small scale and large scale fading variations around signal's mean power.

We define the *coverage area* of a node as area around this node where the received mean power of transmitted signals from the central node is higher than or equal to a threshold value  $\gamma$ . With the power law model for radio propagation, the coverage area is circular with radius  $R$ . It is realistic to assume that  $\gamma$  is equal to the receiver sensitivity<sup>3</sup>. A node can have direct communication with all nodes that fall inside its coverage area.

<sup>2</sup>Path loss exponents obtained based on measurements in different mobile radio environments are shown in the following table [15]:

Environment	Path loss exponent, $\eta$
free space	2
urban area	2.7 to 3.5
shadowed urban area	3 to 5
in building (obstructed)	4 to 6

<sup>3</sup>A realistic value for  $\gamma$  in Wireless LAN systems is -82 dBm.

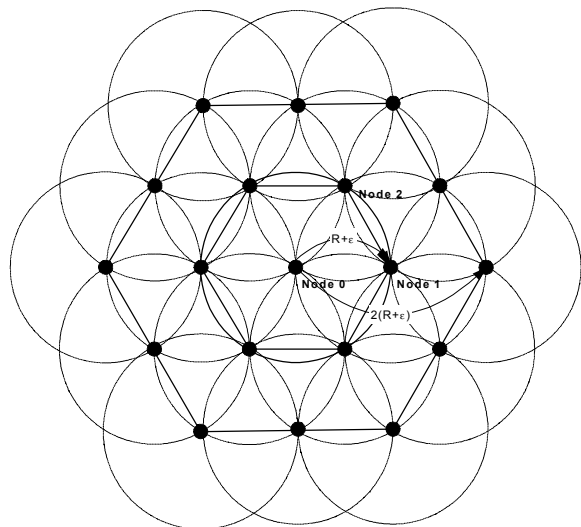


Fig. 1. interfering nodes closest to node 0, when basic form of carrier sensing with collision avoidance is used.

2) *Medium Access Control (MAC)*: We assume that on the data link layer, the ad-hoc network uses a multiple access scheme with carrier sensing. Carrier Sense Multiple Access with Collision Avoidance (CSMA/CA) is an example. In the basic form of medium access in CSMA/CA, nodes that overhear each other will not transmit simultaneously [14]. When a node, say node 0, is transmitting there will be no interference from other nodes inside the coverage area of node 0. In the worst case situation, the first set of interfering signals will come from signals transmitted from nodes just outside the coverage area of node 0 (at distance  $R + \epsilon$  to node 0). For example, in Figure 1 the first interfering signal could originate from node 1. When node 0 and node 1 are transmitting simultaneously, the next interfering signal could only come from nodes outside the coverage areas of both these nodes. Node 2 at the crossing point of two circles with radius  $R + \epsilon$  in Figure 1 could be the second interference source. Adding new interfering nodes in this way produces the constellation of nodes shown in Figure 1, with node 0 in the center of the constellation. As depicted in this figure, there are at most 6 interfering nodes at distance  $R + \epsilon$  to node 0. On the next interfering ring at distance  $2(R + \epsilon)$ , there are at most 12 interfering nodes. This maximum number of interfering nodes will be taken into consideration in section II-A.3 where we choose a lattice form to represent the ad-hoc network.

3) *Uniform distribution of nodes*: Our model assumes uniform distribution of nodes over a two-dimensional area with limited size, but larger than the coverage area. We call that area the *service area* of the ad-hoc network. Normally inside the service area any position (x- and y-coordinate) is equally probable to be occupied by a mobile node. However, in our approach we simplify this by introducing a regular lattice to which the position of mobile nodes is restricted. It will be shown in section V how this restriction regarding the permissible positions for mobile nodes enables the estimation of the expected value of  $C/I$ , without having accurate knowledge about movement patterns and exact location of all nodes at any moment.

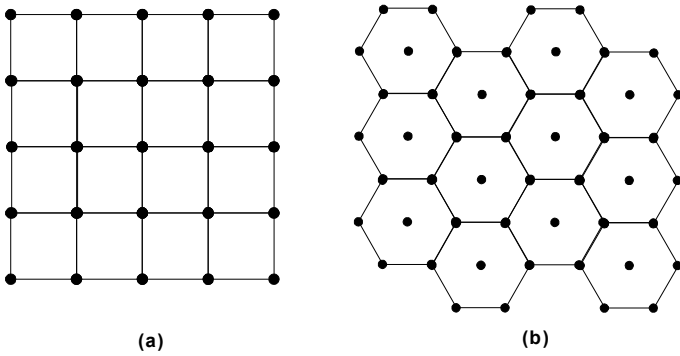


Fig. 2. Nodes uniformly positioned on a (a) rectangular lattice, (b) hexagonal lattice (honey grid)

Introducing a regular lattice can be seen as enforcing a certain granularity on the two-dimensional plane for the position of mobile nodes. On this lattice each node has a number of *adjacent* nodes, that we define as nodes in direct vicinity and with the same distance to that node. When all positions on a regular lattice are occupied, all nodes that are not at the borders of the service area should have the same number of adjacent nodes; and adjacent nodes should be at the same distance from each other. Geometrically, two lattices fulfill these requirements. These lattices are the rectangular lattice and the hexagonal lattice shown in Figure 2. In mobile ad-hoc networks communication between nodes takes place over radio channels and each node may have direct communication with all nodes inside its coverage area. It should be noticed that, depending on the transmission power and radio propagation conditions, the coverage area of a node may contain more nodes than its adjacent nodes.

From the two lattices shown in Figure 2 we have chosen in this paper to base our model on the hexagonal lattice. In this model, that we for obvious reasons will call the honey-grid model, the permissible positions of nodes on the lattice overlap perfectly with the position of interfering nodes in the maximum interference constellation shown in Figure 1. Therefore, the honey-grid model is most suitable for studying interference effects under *worst case* conditions, because it allows for the maximum number of interfering signals to be taken into account when carrier sensing is used for medium access.

4) *Homogeneity*: We assume all nodes transmit with the same power. Further, all nodes have the same traffic generation behavior and all data has the same priority.

### B. Model parameters

From the view point of the center node in a honey-grid lattice, as illustrated in Figure 3, other nodes are positioned on co-centered hexagons. We call each of these hexagons a *ring*. The first hexagonal ring has a side of size  $\Delta$ , and contains 6 nodes. The  $i^{th}$  hexagonal ring has a side of size  $i\Delta$  and contains  $6i$  nodes. The size of the network can be expressed in terms of  $k$  co-centered hexagonal rings around node 0, or by  $N$  the total number of node in this configuration.  $N$  and  $k$  are linked through the formulas:

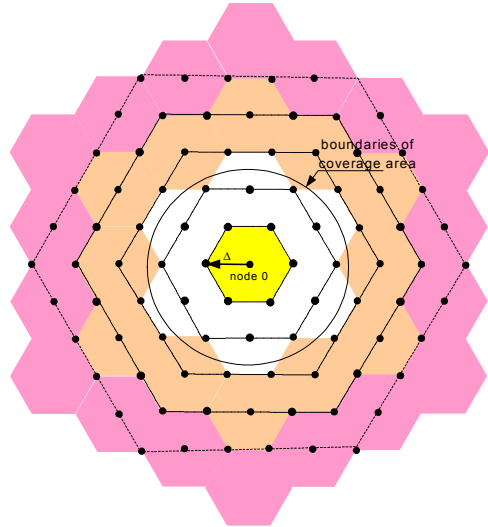


Fig. 3. The honey-grid model showing all nodes.

$$N = 1 + \sum_{j=1}^k 6j = 1 + 3k(k+1), \quad (2)$$

$$k = \left\lceil \sqrt{1/4 + (N-1)/3} - 1/2 \right\rceil$$

where the sign  $\lceil x \rceil$  indicates rounding up to the nearest integer (because the last hexagonal ring may be partially filled).

In Figure 3 we have depicted the coverage area for node 0 in the center of the configuration. The number of nodes inside the coverage area of each node is called the node's *degree*, and is indicated by  $n$ . We assume that an entire ring is either included or excluded from the coverage area. We define a node's *reach* as the number of hexagonal rings that fall inside the coverage area of that node. We indicate the reach of a node by symbol  $a$  (for example,  $a = 2$  in Figure 3). The degree of a node that is not at the borders of the service area is

$$n = \sum_{j=1}^a 6j = 3a(a+1). \quad (3)$$

Each node may communicate directly with all nodes inside its coverage area. For reaching other destinations multi-hopping must be used. There are basically two ways for reaching each destination: If node 0 in Figure 3 wishes to communicate with a node positioned on ring 3, it either can hop through a node on ring 1 and then a node on ring 2; or it can skip ring 1 and hop directly to a node on ring 2 before reaching the destination. The first method preserves energy while the second method keeps the number of hops minimum. We will show that our model can work with both routing methods.

If we consider minimum hop routing, certain intermediate rings on the way from source to destination can be skipped. Figure 4 shows in tick lines the subset of rings that can be used for multi-hop routing to any destination. We will call these rings *relay rings*. When packets are routing throughout the network, there may be multiple paths to the same destination. For example, the source (node 0) and the destination (node 3) shown

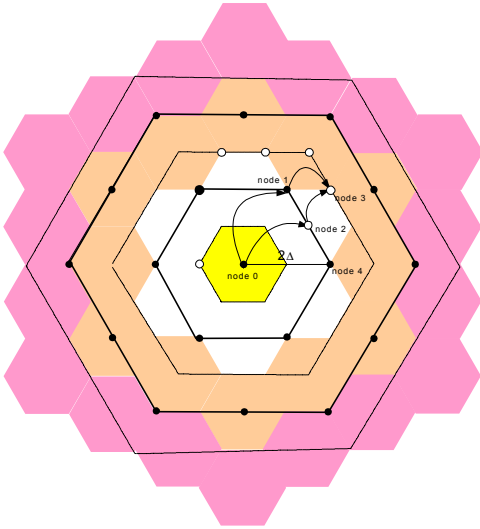


Fig. 4. Relay rings and relay nodes in a honey-grid. Thick lines show relay rings, and dark circles show relay nodes. Hollow circles are other nodes in the network.

in Figure 4 may be connected by the path going through nodes 0-1-3 or the path going through nodes 0-2-3. In our calculation of interference it is important to know the amount of relay traffic caused by multiple hops from source to destination, but the exact path from source to destination is not relevant. Therefore, for us both these paths are the same as they both consists of two hops. In Figure 4 where  $a = 2$ , we see that the first relay ring has a side of the size  $2\Delta$  and contains 6 relay nodes. Relay nodes are those nodes on each relay ring that need to be used to reach any arbitrary destination (for example, when nodes 1 and 4 are relay nodes, node 2 is not chosen as relay node because all destinations that could be reached through node 2 are already reachable through either node 1 or node 4). Generally, if  $a$  is the reach of node 0, the number of co-centered relay rings seen from node 0 is  $\lfloor k/a \rfloor$ , where the sign  $\lfloor x \rfloor$  indicates rounding down to the nearest integer. The number of relay nodes (source node included) is then:

$$N_r = 1 + \sum_{j=1}^{\lfloor \frac{k}{a} \rfloor} 6j = 1 + 3 \left\lfloor \frac{k}{a} \right\rfloor \left( \left\lfloor \frac{k}{a} \right\rfloor + 1 \right). \quad (4)$$

We mentioned earlier in this section that our model can handle energy efficient routing as well as minimum hop routing. If parameter  $a$  is chosen to equal 1, regardless of the reach of mobile nodes, the hopcount (see section III), traffic estimation (see section IV) and carrier to interference ratio (see section V) are found for energy efficient routing. If parameter  $a$  is chosen equal to the maximum radio reach of mobile nodes, the hopcount, traffic estimation and carrier to interference ratio are found for minimum hop routing.

### III. HOPCOUNT IN THE HONEY-GRID MODEL

For the honey-grid model with parameters  $k$  and  $a$ , the exact number of hops needed to reach from any source node any destination node is computed. The method of computation is

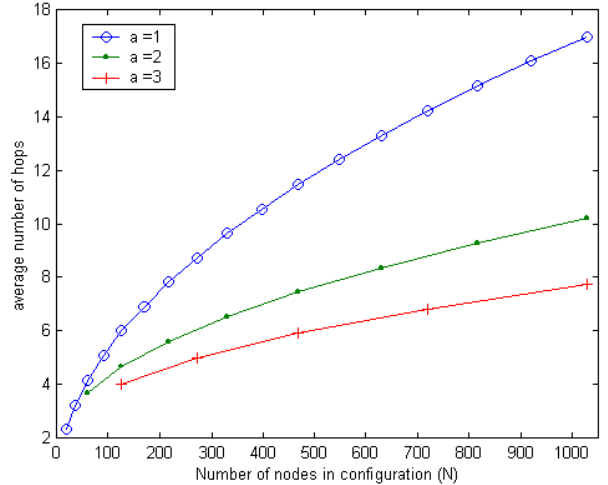


Fig. 5. Mean value of the hopcount in a honey-grid structure for different number of nodes ( $N$ ) and different values of  $a$  ( $a$  node's reach).

explained in the Appendix. From the exact hopcount distribution, the mean and the variance of the hopcount are derived in, respectively, (13) and (14) (see Appendix).

The average hopcount in the entire network for the case that  $a = 1$  is found directly by (13). However, in the case that  $a \neq 1$ , (13) produces the average hopcount over relay nodes. We assume a node that is not situated on a relay ring will hop its traffic first to a relay node positioned on a relay ring. Consequently, if both the source and the destination nodes are not on relay rings, the average hopcount from source to destination is two hops more than the average value found over relay nodes. The average hopcount is then approximately:

$$E[h] \simeq 0.53N_r^{0.5} + 2 \left( 1 - \frac{N_r}{N} \right). \quad (5)$$

In this formula,  $N$  is the number of nodes in the configuration,  $N_r$  (see (4)) is the number of nodes on the relay rings seen from the center and  $(1 - N_r/N)$  represents the probability that either the source or destination node is not a relay node.

Figure 5 shows the mean value of the hopcount calculated with (5) for different number of nodes in a honey-grid structure.

The mean-hopcount determines the expected traffic load in the entire network, as will be explained in the next section.

### IV. TRAFFIC PER NODE

The amount of interference in an ad-hoc network is directly related to the traffic produced per node. This traffic consists of the node's own traffic that is generated by the host connected to the mobile node (we will call this traffic new traffic) and the traffic that the node relays for other nodes. Because of relay traffic, the total amount of traffic per node is strongly related to the multi-hop characteristics of the ad-hoc network. In this section we compute the average total amount of traffic per node. Our basic assumption here is that the new traffic generated by the hosts connected to mobile nodes is Poisson distributed and occurs independent from each other. All hosts are similar and

have the same traffic generation behavior. In other words, mean generated new traffic per host per time interval is the same for all hosts. We denote the mean value of new traffic per time-slot per node by  $\lambda$ .

Consider two nodes  $i$  and  $j$ . When the average hopcount is  $E[h]$ , there are in average  $E[h] - 1$  relay nodes between any source and any destination. Node  $i$  may be a relay station for node  $j$  with the probability  $(E[h] - 1)/(N - 1)$ , and the expected value for relay traffic arriving at node  $i$  from node  $j$  is then  $\lambda(E[h] - 1)/(N - 1)$ . Any node in the ad-hoc network may be a relay node for  $N - 1$  other nodes. Therefore, the expected amount of relay traffic at any node is:  $\lambda(E[h] - 1)$ . The average total traffic per node,  $\Lambda$ , is the sum of the node's own traffic,  $\lambda$ , and all relay traffic that reach that node:

$$\begin{aligned}\Lambda &= \lambda + \lambda(E[h] - 1) \\ &= \lambda E[h].\end{aligned}\quad (6)$$

In this formula,  $E[h]$  is the expected value of the hopcount which is found through (5).

## V. INTERFERENCE CALCULATION

In this section we find a formula for computation of the amount of interference that could be experienced by users in a wireless ad-hoc network.

With uniform distribution of nodes, each node has  $n$  other nodes inside its coverage area (except for nodes at the borders of the network). As explained in section II, around node 0 the first set of interfering signals will come from signals that are transmitted from nodes just outside the coverage area of node 0. Recalling our assumption that an entire ring is either included or excluded from the coverage area, the first ring of interference consists of 6 nodes positioned at distance  $(a + 1)\Delta$  to node 0. Generally, if  $a$  is the reach of node 0, the number of co-centered interference rings seen from node 0 is  $\lfloor k/(a + 1) \rfloor$ , and the number of interfering nodes is:

$$N_i = \sum_{j=1}^{\lfloor \frac{k}{a+1} \rfloor} 6j = 3 \left\lfloor \frac{k}{a+1} \right\rfloor \left( \left\lfloor \frac{k}{a+1} \right\rfloor + 1 \right). \quad (7)$$

Figure 6 shows interfering rings and interfering nodes observed from the centre node in a honey-grid model with  $a = 1$ .

Nodes in the center of the configuration have the highest number of potential interfering nodes around them in all directions. Therefore, we choose the amount of interference experienced at node 0 as representative for the maximum level of interference inside this network. In the remainder of this section, a closed expression for interference at node 0 is derived. If the level of interference is acceptable at node 0, we can assume that it is also acceptable for other nodes.

To calculate the amount of interference experienced at node 0, we add the interference power received at node 0 from all interfering nodes. The first interference ring contains 6 nodes at distance  $(a + 1)\Delta$ . The second interference ring consists of 12 interfering nodes from which 6 nodes in the corners of the hexagonal ring are at distance  $2(a + 1)\Delta$  to node 0 and 6

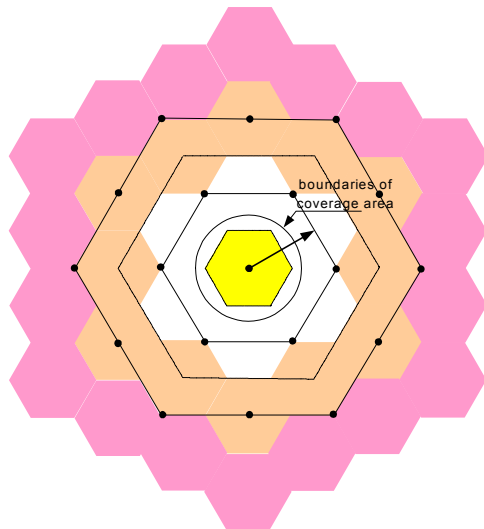


Fig. 6. Honey-grid with interfering rings (thick lines) for  $a = 1$ .

other nodes are at distance  $\sqrt{3}(a + 1)\Delta$  to node 0. The distance of nodes on each ring to node 0 can be calculated exactly. However, in our calculations in this paper we use a simplification: we assume that the distance between all interfering nodes on each ring to node 0 is equal to the distance of the corner nodes to node 0. This is not an inaccurate approximation, especially when the service area is large. The  $j^{th}$  interference ring contains  $6j$  nodes at approximated distance  $j(a + 1)\Delta$  to node 0. Let  $q$  be the probability of transmission (transmission of own signals or relay signals) per node. Using (1), the mean power of interfering signals originating from ring  $j$  is  $6jqc(j(a + 1)\Delta)^{-\eta}$ . The total amount of interference mean power is then:

$$I = 6qc((a + 1)\Delta)^{-\eta} \sum_{j=1}^{\lfloor \frac{k}{a+1} \rfloor} j^{-(\eta-1)}. \quad (8)$$

When network size increases  $\lfloor \frac{k}{a+1} \rfloor \rightarrow \infty$ , and the above formula can be written as:

$$I_\infty = 6qc((a + 1)\Delta)^{-\eta} \zeta(\eta - 1)$$

where for  $\text{Re}(s) > 1$ ,  $\zeta(s) \triangleq \sum_{j=1}^{\infty} j^{-s}$  is the Riemann-Zeta function [18]. When the path loss exponent  $\eta > 2$ ,  $\zeta(\eta - 1)$  is a converging series with positive terms and is upper-bounded by [19]:

$$\sum_{j=1}^{\infty} j^{-(\eta-1)} \leq 1 + \int_1^{\infty} \frac{1}{x^{\eta-1}} dx = \frac{\eta - 1}{\eta - 2}.$$

Based on the above formula we can conclude that the amount of interference power in a mobile ad-hoc network with CSMA/CA protocol for multiple access control is upper-bounded by the following expression:

$$I \leq 6qc((a + 1)\Delta)^{-\eta} \frac{\eta - 1}{\eta - 2}. \quad (9)$$



This conclusion is an important result. In section VII we will discuss that this conclusion is valid for all ad-hoc networks with moving nodes.

For correct reception of radio signals, the carrier to interference ratio  $C/I$  needs to be higher than a certain threshold value (for example 7 dB).  $C/I$  is the ratio between the mean power of wanted signal and the mean power of the sum of interfering signals. In the honey-grid model the lowest expected value for wanted signal power,  $C$ , is related to the situation that the wanted signal (signal from the source) is transmitted from the farthest neighbor of node 0 at distance  $a\Delta$ . The highest value of  $C$  is related to the situation that wanted signal is transmitted from the nearest neighbor of node 0, which is at distance  $\Delta$ . The expected value for  $C$  is found then by taking into account all possible positions of the wanted signal transmitter:

$$\begin{aligned} E[C] &= \sum_{j=1}^a \frac{6j}{3a(a+1)} c \cdot (j\Delta)^{-\eta} \\ &= \frac{2c\Delta^{-\eta}}{a(a+1)} \sum_{j=1}^a j^{-(\eta-1)}. \end{aligned}$$

In mobile ad-hoc networks based on W-LAN technologies, mostly spread-spectrum techniques are used. In these cases we should only consider the amount of interference power that coincides with the wanted signal after de-spreading process. The reduction in interference power is indicated by "processing gain"<sup>4</sup>,  $g$ . Based on the above formula and (8), the following formula calculates the expected value of  $C/I$  for a node in the center of an ad-hoc network.

$$\begin{aligned} E[C/I] &= \frac{\frac{2c\Delta^{-\eta}}{a(a+1)} g \sum_{j=1}^a j^{-(\eta-1)}}{6qc((a+1)\Delta)^{-\eta} \sum_{j=1}^{\lfloor \frac{k}{a+1} \rfloor} j^{-(\eta-1)}} \\ &= \frac{g \sum_{j=1}^a j^{-(\eta-1)}}{3a(a+1)^{-(\eta-1)} q \sum_{j=1}^{\lfloor \frac{k}{a+1} \rfloor} j^{-(\eta-1)}}. \end{aligned}$$

From the above formula we see that the expected value of carrier to interference ratio,  $E[C/I]$ , depends on the network size  $k$ , density of the network  $a$ , path-loss exponent  $\eta$  and the probability of transmission per node  $q$ . The later depends directly on the mean value of generated traffic per node  $\Lambda$  (see (6)). Because we assumed a Poisson arrival process for traffic per node, for  $q$  we can write:

$$\begin{aligned} q &= 1 - e^{-\Lambda} \\ &= 1 - e^{-\lambda E[h]}. \end{aligned}$$

Substituting  $q$  in the above formula gives:

$$E[C/I] = \frac{g \sum_{j=1}^a j^{-(\eta-1)}}{3a(a+1)^{-(\eta-1)} (1 - e^{-\lambda E[h]}) \sum_{j=1}^{\lfloor \frac{k}{a+1} \rfloor} j^{-(\eta-1)}}. \quad (10)$$

<sup>4</sup>In 802.11 DSSS (Direct Sequence Spread Spectrum) the processing gain is realized by modulating each data bit with an 11 bit Barker code (pseudo random sequence). Processing gain is therefore 11:1, or 10.4 dB [14].

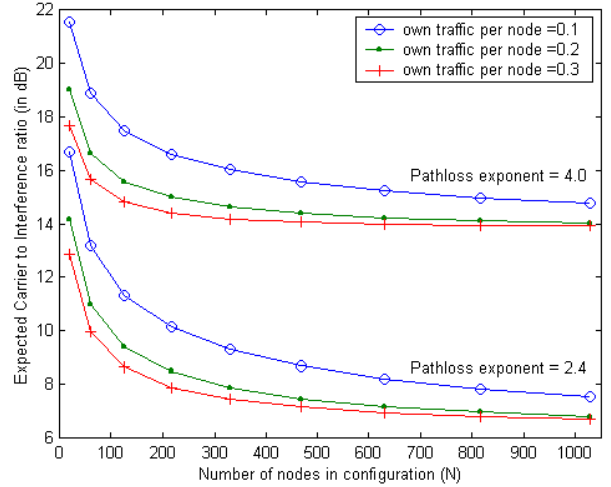


Fig. 7. Expected value of  $C/I$  for a node in the center of a honey-grid structure for different values of a node's own traffic,  $\lambda$ . In all cases the node's reach,  $a$ , is 1 and the processing gain is 10.4 dB.

Here,  $\eta$  is the path loss exponent,  $g$  is processing gain,  $a$  is the reach of nodes in the center of the configuration,  $k$  is the number of rings in the network (size of the network),  $\lambda$  is the mean arrival rate of new packets per node per time-slot (node's own traffic) and  $E[h]$  is the average number of hops which is found by (5).

#### A. Effect of network size and network density on $C/I$

Figure 7 shows the calculated values of  $E[C/I]$  according to (10) for different values of path loss exponent and different number of nodes with  $a = 1$ . Figure 8 shows the calculated values of  $E[C/I]$  according to (10) for a fixed value of path loss exponent and the node's own traffic but with different values for  $a$ . From these two figures we can conclude that for large networks the expected value of  $C/I$  tends to an asymptotic value that depends only on the path loss exponent and the value of  $a$ . In other words, for large ad-hoc networks, the expected value of  $C/I$  depends on the network density (which is directly related to  $a$ ) and the path loss exponent. In indoor environments, with higher values of path loss exponent, an ad-hoc network performs better than in outdoor environments where due to lower path loss values radio signals travel to farther distances and cause more interference. Previously in (9) we showed that interference is upper bounded in ad-hoc networks that use carrier sensing for medium access. When interference is upper-bounded we expect  $E[C/I]$  to be under-bounded. Results shown in Figures 7 and 8 confirm this claim.

#### B. Effect of routing overhead on $C/I$

New traffic per node,  $\lambda$ , consists of two parts: the data traffic and routing overhead. Data traffic is the actual communication data to be transmitted from a source to a destination (for example the content of an e-mail). Routing overhead consists of all traffic generated by a node for finding new routes, or for keeping routing information up-to-date. We can use (10) to

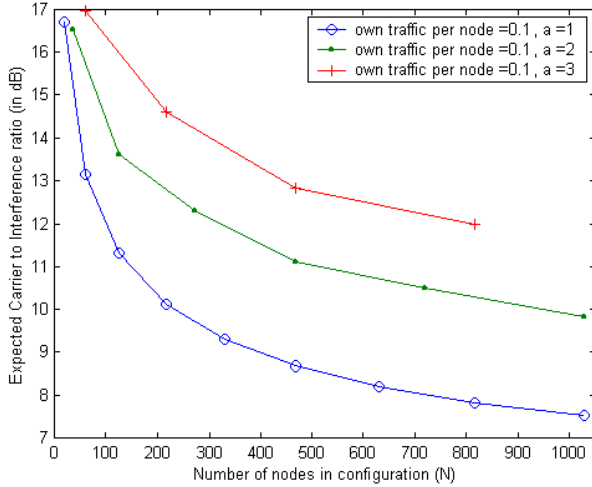


Fig. 8. Expected value of  $C/I$  for a node in the center of a honey-grid structure for different values of a node's reach,  $a$ . In all cases the path loss exponent is 2.4, the node's own average traffic rate is 0.1 packets per time slot and the processing gain is 10.4 dB.

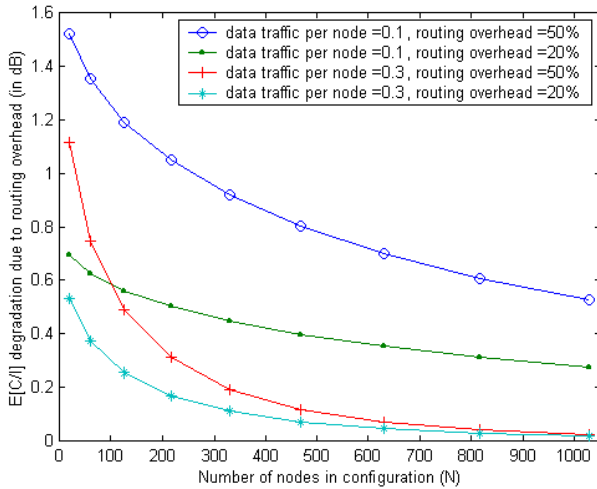


Fig. 9. Effect of traffic increase due to routing overhead on  $E[C/I]$  in an ad-hoc network with different number of nodes. In all cases  $a = 1$ ,  $\eta = 2.4$ , and processing gain is 10.4 dB.

study the effect of traffic increase due to routing overhead on the performance of a mobile ad-hoc network. Figure 9 shows calculated results for a few examples. In this figure, degradation of  $E[C/I]$  along the y-axis is the difference between  $E[C/I]$  with routing overhead and  $E[C/I]$  for the same value of data traffic with zero routing overhead. From Figure 9 we may conclude that routing overhead does not seem to have significant influence on  $E[C/I]$  in large networks with high data traffic volumes.

## VI. CAPACITY AND THROUGHPUT

Having access to the expected values of  $C/I$ , we can use the Shannon channel capacity formula [21, Chapter 5] to find an upper bound on reliable data transmission speed between two

neighboring nodes in the ad-hoc network<sup>5</sup>. When the expected value of  $C/I$  decreases, capacity of the link between two nodes calculated with Shannon formula decreases as well. An additional restriction on capacity is imposed by the MAC protocol. In the basic form of CSMA/CA at any moment in time only one of the neighboring nodes may transmit. With node degree  $n$ , the channel capacity needs to be divided by  $n + 1$  to obtain the capacity,  $R_{\max}$ , per node:

$$R_{\max} = \frac{B}{n + 1} \log_2(1 + E[C/I]). \quad (11)$$

Here  $B$  is the channel bandwidth<sup>6</sup> in Hz,  $n$  is the node's degree and  $E[C/I]$  is the expected carrier to interference ratio found by (10).  $R_{\max}$  is in bits per second and indicates the upper bound on the time-averaged error free bit transmission speed per node.

In this paragraph we intend to compare the output bit rate per node to  $R_{\max}$  for different network sizes, different network densities and different values of input data bit rate per node. Based on (6) we can find the relation between the input bit rate per node,  $R_{in}$ , and the output bit rate per node,  $R_{out}$ . However, for translation from packets per time-slot to bits per second we need the exact duration of a time-slot and the amount of overhead within each time slot. Let us indicate duration of each time-slot by  $t_{ts}$ . Each time-slot consists of an overhead part,  $t_o$ , and a useful data transmission part,  $t_d$ . In other words  $t_{ts} = t_o + t_d$ . The overhead time is the time needed for transmission of preamble and header in each data frame. Further, the overhead time includes the required inter-frame spacing times and the required time for the reception of MAC Acknowledgments for each data frame. A typical value for  $t_o$  in IEEE 802.11b is  $364 \mu s$  [14]. The length of  $t_d$  depends on data packet size,  $P$ , and data transmission speed,  $r$ . We can write  $t_d = P/r$ . In IEEE802.11b,  $P$  may vary between 34 to 2346 bytes, while  $r$  is either 1 Mbps, 2 Mbps, 5.5 Mbps or 11 Mbps [14]. The input bit rate per node,  $R_{in}$ , and the output bit rate per node,  $R_{out}$ , relate to  $\lambda$  and  $\Lambda$  as:

$$R_{in} = \frac{\lambda P}{t_{ts}},$$

$$R_{out} = \frac{\Lambda P}{t_d} = \frac{E[h]\lambda P}{t_d} = E[h]R_{in} \frac{t_{ts}}{t_d}. \quad (12)$$

We can use (11) and (12) to compute the available capacity and the required output bit rate per node when network size, network density and input traffic per node change. Figures 10 and 11 show two examples. In these figures we see when network size increases the output bit rate generated per node increases as well. On the other hand, by increasing network size the amount of interference increases and this will cause the

<sup>5</sup>The classic Shannon formula is derived assuming a channel with white Gaussian noise. Here we use this formula with  $C/I$  because after despreading process in DSSS systems interference within the wanted signal bandwidth has noise-like characteristics.

<sup>6</sup>Because  $E[C/I]$  is the expected value of carrier to interference ratio after despreading of CDMA signals, the channel bandwidth,  $B$ , is also the channel bandwidth after despreading process. In IEEE802.11b the radio channel bandwidth before despreading is 22 MHz. With a processing gain of 11,  $B$  is equal to 2 MHz. For more information see [22].

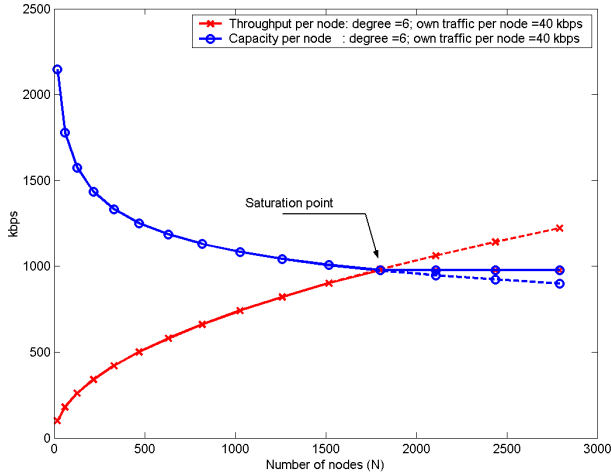


Fig. 10. Comparing capacity and required output bit rate per node. In this figure the node's reach,  $a$ , is 1 (6 neighbors per node) and each node's own traffic equals to 40 kbps. For calculations we have assumed: channel bandwidth,  $B$ , is 22 MHz (before despreading of CDMA signals), data packets size,  $P$ , is 1000 bytes, transmission speed,  $r$ , is 2 Mbps,  $t_0 = 364\mu s$  and the pathloss exponent is 2.4.

available capacity per node to decrease. At the point where the increasing output bit rate intersects with the decreasing capacity per node, we say that the *network saturation point* is reached<sup>7</sup>. Beyond this point a node will not have time for successful transmission of any additional incoming data. As a result, the useful output bit rate per node, i.e. throughput per node, remains at a constant level even when the network size or the input data rate increase. Beyond the saturation point, increasing network size or input data rate will not increase the throughput but will cause the delay to grow.

An other effect visible from comparing figures 10 and 11 is the effect of increase in network density. When network density increases, number of neighbors per node increases as well. We see when the network density increases (higher node's degree in Figure 11), the network saturation point is reached for lower number of nodes and at lower data rates.

We mention here that the flattening of throughput in IEEE802.11b networks when the traffic load is increased has already been observed in some experimental measurement results [23]. We believe our model for calculation of throughput per node could have practical application in the design and optimization of ad-hoc networks and sensor networks. Figure 12 illustrates an other set of data obtained by using (11) and (12) to compute the throughput per node for different number of nodes and different values of input bit rate per node. From this figure we can read the maximum supported input bit rate per node for different network sizes.

## VII. MODEL ASSESSMENT

In mobile wireless ad-hoc networks nodes may move freely inside the whole service area. Our introduction of the regular

<sup>7</sup>In figures 10 and 11 the dashed lines show the trend in increase of the output bit rate and decrease in the available capacity if saturation point was not reached.

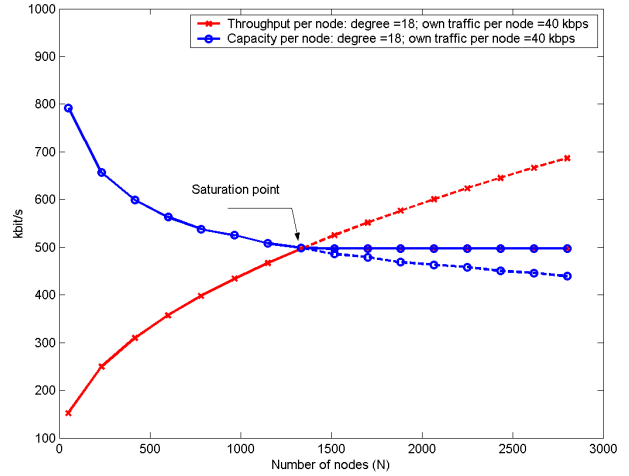


Fig. 11. Comparing capacity and required output bit rate per node. In this figure the node's reach,  $a$ , is 2 (18 neighbors per node). Other assumptions are the same as in Figure 10.

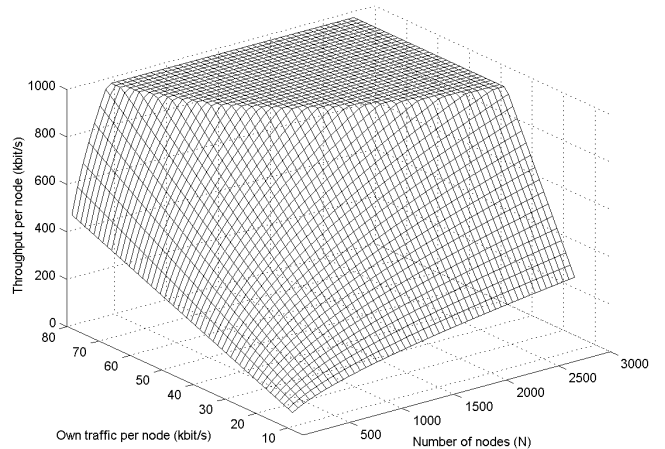


Fig. 12. Throughput per node for different values of input data bit rate per node and different number of nodes. Each node's own traffic varies between 10 kbps and 80 kbps. Other values and assumptions are the same as in Figure 10.

honey-grid lattice seems to contradict this freedom of movement. Therefore, the question may be raised whether our model can cope with moving nodes.

Our main purpose in this paper is to estimate the expected levels of interference in mobile ad-hoc networks. In particular, we showed in section V that interference in wireless mobile ad-hoc networks is upper-bounded. By increasing or decreasing the size of hexagons in our model we are able to cope with low or high density of nodes, but we do not model movement of nodes. However, our calculations of  $E[C/I]$  remain valid as long as uniform node distribution is not affected by moving nodes. Even when uniform distribution of nodes is disturbed; with the medium access control scheme assumed in this paper, the *maximum* number of interfering nodes and their relative position would have to match the constellation of interfer-



ing nodes discussed in section II-A.2. Therefore, concerning the maximum number of interfering signals and the maximum amount of interference, our computations are not affected by moving nodes.

In our calculation of interference we have taken into account the expected amount of relay traffic per node, which is found based on the exact hopcount distribution over the honey-grid. Deviation from the uniform node distribution could affect the hopcount, and consequently the total amount of traffic per node. The effect of this point on  $C/I$  calculations requires further investigation. However, regardless of the total traffic per node, the probability of transmission per node,  $q$  in (9), can never exceed 1. Hence, we still may conclude that interference in mobile ad-hoc networks remains upper-bounded even when the nodes are not uniformly distributed.

### VIII. CONCLUSIONS

The model proposed in this paper for calculation of interference and capacity in mobile ad-hoc networks takes into account the number of nodes, density of nodes, multi-hop characteristics of the network, and relay traffic. Based on this model we have evaluated effects of network size change, network density change and traffic variation on the expected value of carrier to interference ratio, and consequently the throughput of the network. Our study presented in this paper offers new insights about scalability and optimization of routing protocols for of ad-hoc networks. We summarize the main results here:

- 1) The expected amount of interference in mobile ad-hoc networks that use carrier sensing for medium access is upper-bounded to a value that does not depend on the network size (in terms of the number of nodes). This upper bound for the basic form of CSMA/CA can be computed using (9).
- 2) When the network size increases, the output bit rate generated per node increases until the network saturation point is reached. At this point, increasing network size or input data rate will not increase the throughput but will cause the delay to grow.
- 3) When the network density increases, the average node's degree increases as well. Because more nodes fall within each other's direct reach, the average hopcount is reduced (see Figure 5). As a result, the aggregate relay traffic reduces and carrier to interference ratio improves. On the other hand, due to carrier sensing mechanisms, less nodes are allowed to transmit simultaneously. This could reduce available capacity per node. The combined effect may cause the network saturation point to be reached at lower number of nodes and for lower data input rates. The network saturation point can be found using (11) and (12).
- 4) We have shown that traffic increase due to routing overhead does not affect the expected values of  $C/I$  significantly in large networks with high data traffic volumes (e.g., degradation of the expected value of  $C/I$  is less than 0.8 dB for 20% routing overhead for the values depicted in Figure 9).

### ACKNOWLEDGMENT

This research is supported by the Towards Freeband Communication Impulse of the technology programme of the Ministry of Economic Affairs in The Netherlands.

### REFERENCES

- [1] IETF Mobile Ad-hoc Networks (MANET) Working Group web site, <http://www.ietf.org/html.charters/manet-charter.html>.
- [2] "Optimized Link State Routing Protocol", IETF-draft, IETF MANET Working Group, September 2001.
- [3] "Ad hoc On-Demand Distance Vector (AODV) Routing", IETF-draft, IETF MANET Working Group, January 2002.
- [4] E.M. Royer; C-K. Toh, "A Review of Current Routing Protocols for Ad-hoc Mobile Wireless Networks", IEEE Personal Communications, Volume: 6 Issue: 2, April 1999.
- [5] D.A. Maltz; J. Broch; D.B. Johnson, "Lessons from a full-scale multi-hop wireless ad hoc network testbed" IEEE Personal Communications, Volume: 8 Issue: 1, Feb. 2001.
- [6] C.E. Perkins; E.M. Royer; S.R. Das; M.K. Marina, "Performance comparison of two on-demand routing protocols for ad hoc networks", IEEE Personal Communications, Volume: 8 Issue: 1, Feb. 2001.
- [7] Z.J. Haas; M.R. Pearlman, "The performance of query control schemes for the zone routing protocol", IEEE/ACM Transactions on Networking, Volume: 9 Issue: 4, Aug. 2001.
- [8] Cesar A. Santivanez; Bruce McDonald; Ioannis Stavrakakis; Ram Ramanathan, "On the Scalability of Ad Hoc Routing Protocols", Proceedings IEEE Infocom 2002, pp. 1688-1697.
- [9] K. Bertet; C. Chaudet; I.G. Lassous; L. Viennot, "Impact of interferences on bandwidth reservation for ad hoc networks: a first theoretical study", Global Telecommunications Conference, 2001. GLOBECOM '01. IEEE, Volume: 5, 2001.
- [10] Michael Gastpar; Martin Vetterli, "On The Capacity Of Wireless Networks: The Relay Case", Proceedings IEEE Infocom 2002, pp. 1577-1586.
- [11] Yu-Chee Tseng; Chih-Shun Hsu; Ten-Yueng Hsieh, "Power-Saving Protocols for IEEE 802.11-Based Multi-Hop Ad Hoc Networks", Proceedings of IEEE Infocom 2002, pp. 200-209.
- [12] V. Rodoplu and T.H.-Y. Meng, "Minimum Energy Mobile Wireless Networks," IEEE Journal on Selected Areas in Communications, Vol. 17, No. 8, August, 1999.
- [13] P. Van Mieghem; G. Hooghiemstra; R. W. van der Hofstad, "Scaling Law for the Hopcount", Delft University of Technology, report 2000125, January 2000.
- [14] ANSI/IEEE Std 802.11, 1999 Edition, Part 11: Wireless LAN Medium Access Control (MAC) and Physical Layer (PHY) Specifications.
- [15] T.S. Rappaport, "Wireless Communications, Principles and Practice", Upper Saddle River Prentice-Hall PTR, 2002.
- [16] H.L. Bertoni, "Radio Propagation for Modern Wireless Systems", Prentice-Hall PTR, 2000.
- [17] R. Prasad, "Universal Wireless Personal Communications", Artech House Publishers, 1998.
- [18] M. Abramowitz; I. R. Stegun, "Handbook of Mathematical Functions", Dover Publications, 1970.
- [19] C.H. Edwards, "Calculus : with analytic geometry", Upper Saddle River Prentice-Hall, 1998.
- [20] Wei Ye; John Heidemann; Deborah Estrin, "An Energy-Efficient MAC Protocol for Wireless Sensor Networks", Proceedings of IEEE Infocom 2002, pp. 1567-1576.
- [21] J.M. Wozencraft, I.M. Jacobs, "Principles of Communication Engineering", John Wiley & Sons, 1965.
- [22] J.L. Massey, "Information Theory Aspects of Spread-Spectrum Communications", IEEE Third International Symposium on Spread Spectrum Techniques and Applications, 1994. IEEE ISSSTA '94., Page(s): 16 -21 vol.1
- [23] T. Pagtzis; P. Kirstein; S. Hales, "Operational and fairness issues with connection-less traffic over IEEE802.11b", IEEE International Conference on Communications 2001, Vol. 6, 2001.

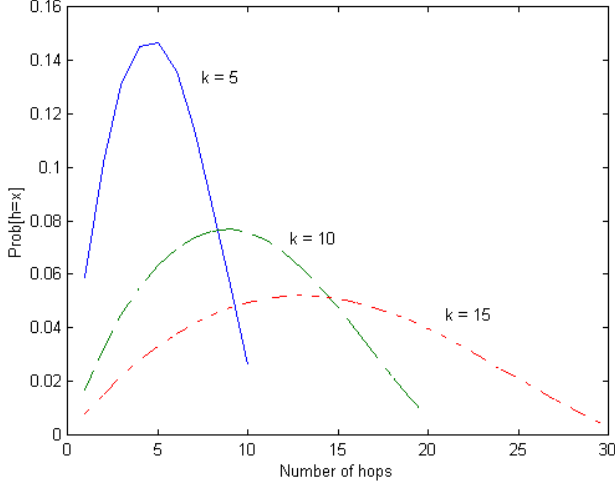


Fig. 13. Hop distribution for  $k=5$  (91 nodes),  $k=10$  (331 nodes) and  $k=15$  (721 nodes). In all cases  $a=1$ .

#### APPENDIX

We have found the exact hop distribution for the honey-grid structure. The mean and the variance are derived directly from the exact distribution of the hopcount.

The method for finding hopcount distribution in the honey-grid model is discovered by finding the exact hopcount for several network configurations (from  $k = 1$  to  $k = 8$ ) and extrapolating the observed systematics to higher values of  $k$ . The algorithm found in this way is presented here.

```

begin
k = number of rings
a = a node's reach
s = k/a [note: s should be an integer, and k>a]
form matrix A(2s, s) with all values zero
form matrix B(2s, s) with all values zero
form matrix C(2s, s) with all values zero
form array h(2s) with all values zero
for j = 1 to s
  A(1, j) = 3
  A(i, j) = A(i-1, j) + 2, for i=2 to j
  A(i, j) = A(i-1, j), for i=j+1 to 2j
  B(i, j) = 2, for i=1 to 2j-1
  B(2j, j) = 2j+1
  A(i, j) = B(i, j)/2 + (A(i, j) - B(i, j)), for i=1 to 2j
  h = h + 6j A(:, j) [note: A(:, j) denotes column j of A]
end for loop
C(1, j) = C(1, j-1) + (j-1), for j=2 to s
C(i, j) = C(i-1, j-1) + C(1, j-1), for i=2 to s-1 and j=i to s
C(i, j) = -C(2j-i+1, j), for j=2 to s and i=j+1 to 2j
h = h + 6C(:, s) [note: C(:, s) denotes column s of C]
end

```

At the end of this procedure, array  $h$  contains the exact number of node combination that are at distance  $1, 2, \dots, 2(k/a)$  hops from each other. As an example, Figure 13 shows the distribution of hopcount for three different values of  $k$ . In all cases it is assumed that  $a = 1$ .

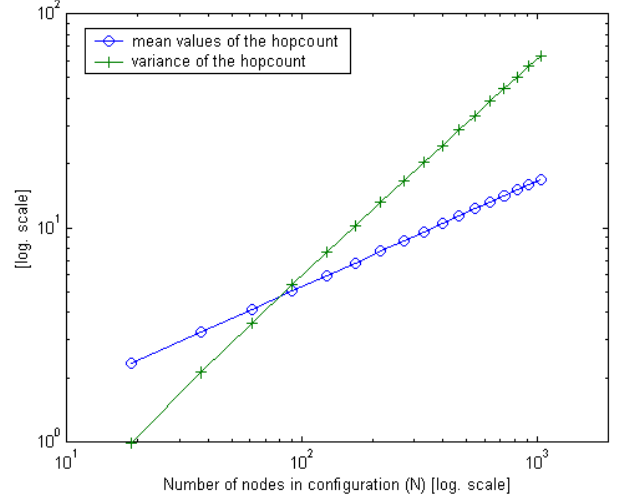


Fig. 14. Mean and variance of the hop count. Results are found through the procedure for finding exact hop distribution in honey-grid model.

When  $a = 1$ , this calculation method produces the exact number of hops from any source to any other destination in the entire network. We have used the above described procedure to find the mean and variance of hopcount for different number of nodes  $N$ . The results, in logarithmic scale, are shown in Figure 14.

As observed in this figure, on logarithmic scale, the mean and the variance of the hopcount seem to be linear functions of the number of nodes. This is confirmed by first order curve fitting results:

$$\begin{aligned} \ln E[h_N] &\simeq 0.50 \ln(N) - 0.64 \\ \ln \text{var}[h_N] &\simeq \ln(N) - 2.81 \end{aligned}$$

These linear approximations fit almost perfectly with computed values<sup>8</sup>. Based on these formulas we find the following approximation for the average and variance of the hopcount:

$$E[h_N] \simeq 0.53 N^{0.5} \quad (13)$$

$$\text{var}[h_N] \simeq 0.06 N \quad (14)$$

It is interesting to mention that the formulas found here for the mean and the variance of the hopcount in honey-grid model are in-line with expressions found in [13] for *rectangular* d-lattice graphs. For the 2-dimensional lattice  $d = 2$  in [13] we find;  $E[h_N] \simeq 2/3 N^{1/2}$ , and  $\text{var}[h_N] \simeq 1/9 N$ . In comparison to (13) and (14) only the prefactor due to a form difference between a hexagonal and rectangular lattice is slightly different. It should be noticed that (13) and (14) are valid for small as well as large values of  $N$ , while expressions in [13] are found for large values of  $N$ .

<sup>8</sup>For  $k = 500$ , the root mean square error (rmse) of the linear fit for the average hopcount is of the order  $10^{-4}$ , and the rmse for the linear fit of the variance is of the order  $10^{-3}$ .